C. R. Physique 15 (2014) 563–572

Contents lists available at ScienceDirect

Comptes Rendus Physique

www.sciencedirect.com

Emergent phenomena in actinides / Phénomènes émergents dans les actinides

NMR studies of actinide oxides – A review

Le point sur les études des oxydes d'actinides par RMN

Russell E. Walstedt [a,*], Yo Tokunaga [b], Shinsaku Kambe [b]

[a] *Physics Department, The University of Michigan, Ann Arbor, MI 48109, USA*
[b] *Advanced Science Research Center, Japan Atomic Energy Agency, Tokai, Ibaraki 319-1195, Japan*

ARTICLE INFO

Article history:
Available online 16 July 2014

Keywords:
Actinide oxides
Multipolar order
Nuclear magnetic resonance

Mots-clés :
Oxydes d'actinides
Ordre multipolaire
Résonance magnétique nucléaire

ABSTRACT

In this paper, we offer a brief review of the ground-state properties of the cubic oxides AnO_2, where An = U, Np, Pu and Am, as revealed mainly by NMR studies of the $^{17}O^{2-}$ ligand. For PuO_2, where the ground state is a nonmagnetic singlet eigenstate of the cubic crystal field, only the ^{239}Pu has been studied, in a recent breakthrough observation of this elusive isotope [1]. For UO_2 and NpO_2, the former has an exotic four-sublattice antiferromagnetic (AFM) ground state, while the latter has the first multipolar ground state to be identified among actinide compounds, namely a mixture of octupolar and rank 5 (triakontadipolar) order. On the other hand AmO_2, even with the longest-lived isotope ^{243}Am, becomes disordered so quickly from radiation self-damage that its ground state in a recent study was simply a spin glass, while the actual ground state of the cubic crystalline compound remains obscured by this experimental problem. The emphasis throughout is on how ^{17}O NMR studies complement other experimental data to confirm and verify the known exotic magnetic ground states of AnO_2 systems.

RÉSUMÉ

Dans ce papier, nous passons brièvement en revue les propriétés de l'état fondamental des oxydes cubiques AnO_2, avec An = U, Np, Pu et Am, telles que révélées principalement par les études RMN du ligand $^{17}O^{2-}$. Pour PuO_2, où l'état fondamental dans le champ cristallin cubique est un singulet non magnétique, seul le ^{239}Pu a été mesuré dans une étude récente, qui représente une percée pour ce qui concerne cet isotope d'accès difficile. UO_2 a un état fondamental antiferromagnétique (AFM) exotique à quatre sous-réseaux, tandis que NpO_2 montre le premier état fondamental multipolaire identifié dans un composé d'actinide, consistant en un mélange d'ordre octupolaire et de rang 5 (triakontadipolaire). Par ailleurs, AmO_2, même avec son isotope possédant la plus longue période, ^{243}Am, devient si rapidement désordonné du fait des dommages qu'il subit par auto-irradiation que son état fondamental était simplement, dans une étude récente, un verre de spins, alors que l'état fondamental réel du composé cubique cristallin demeure masqué par cette difficulté expérimentale. L'accent est mis sur la façon dont les mesures RMN sur le

* Corresponding author.
E-mail addresses: walstedt@umich.edu (R.E. Walstedt), tokunaga.yo@jaea.go.jp (Y. Tokunaga), kambe.shinsaku@jaea.go.jp (S. Kambe).

http://dx.doi.org/10.1016/j.crhy.2014.06.007
1631-0705/

noyau ^{17}O complètent les autres données expérimentales pour confirmer et vérifier l'état fondamental, souvent exotique, établi pour les systèmes AnO_2.

1. Introduction

Studies of the low-temperature physics of actinide compounds were greatly stimulated by the observation for the first time – in 1998 – of the NMR of ^{235}U nuclear spins (or of any actinide) in a solid host compound, namely in antiferromagnetically (AFM) ordered UO_2 [2]. This work, combined with a parallel study of ^{17}O NMR in the same compound, led to a very detailed analysis of the low temperature properties of this system [3]. Since that beginning, studies of ^{17}O NMR as well as direct and indirect measurements of actinide NMR properties have been conducted on NpO_2, PuO_2, and AmO_2, yielding a complete panorama of varied and disparate low-temperature behavior for these relatively simple insulating oxide materials, no two of which are alike. The objective of this paper is to provide a succinct, but informative account of these researches to date. The results, we suggest, will provide a cornerstone for the understanding of low-temperature properties of the many actinide and rare-earth systems exhibiting strongly correlated electronic behavior. A brief review of the NMR studies has been published, [4] and a more comprehensive review of multipolar effects in AnO_2 systems has been given by Santini and co-workers [5].

Each AnO_2 compound listed crystallizes in the CaF_2 structure (Fig. 1), so that the An^{4+} ions are subject to a cubic crystal field. Table 1 gives a summary of ionic states, multiplets, and crystal field ground states, as well as nuclear parameters for the four oxides covered here. Crystal field ground state assignments were taken from the references cited in the table. The AnO_2 compounds are all insulators, a mitigating factor that goes a long way toward understanding the behavior of their 5f electrons. One of the principal questions posed for these systems, then, is what sort of magnetic ground state they exhibit. PuO_2, of course, has a 'nonmagnetic' Γ_1 singlet ground state [8], but nonetheless exhibits a substantial ground state Van Vleck paramagnetism [1].[1] An^{4+} atomic magnetic moments are found to possess AFM exchange couplings with their neighbors. Since the fcc lattice that the An^{4+} occupy is famously inhospitable to AFM sublattices, the question of the AnO_2 magnetic ground state is an interesting one. As is spelled out in detail below, NMR and other experimental probes have revealed three strikingly different results for the three systems concerned. These are (i) a four-sublattice type of AFM order in UO_2, (ii) a combination of octupolar and quadrupolar order along with possible rank-5 multipolar order for NpO_2, and finally, (iii) spin glass order for AmO_2. The latter result occurs for a very special reason, having to do with the short half-life of the isotope ^{243}Am used (see Table 1). In this review, we give particular emphasis to how the studies conducted verify in detail the nature of these ground states.

Regarding the observation of actinide nuclear resonance directly, this is generally a challenging proposition. The reason for this is the enormously large 5f-shell HF coupling constants for the actinides. As a result, normal magnetic fluctuations will tend to make T_1 and/or T_2 unobservably short. Success is therefore most likely at low temperatures. But there, magnetic ordering will often generate internal hyperfine frequency splittings up into the GHz range. In spite of these general expectations about actinide NMR, special circumstances have made it possible to observe the ^{235}U and ^{239}Pu NMR signals directly, and the ^{237}Np NMR indirectly, and to study them extensively. How this came about will be described in some detail in sections below on individual compounds.

2. A study of exotic AFM order in UO_2

^{235}U was the first actinide NMR signal to be observed directly in a solid compound [3]. ^{235}U possesses one of the smallest gyromagnetic ratios (see Table 1) of all naturally occurring nuclei, a factor that helped to make its T_1 long enough at very low temperatures for NMR to be observed. The smallness of γ_{235} and the low natural abundance of ^{235}U might have rendered the nuclear spin-echo signal too small to observe, but two factors have combined to overcome this problem: (i) the possibility of isotopically enriching the sample to greater than 90% ^{235}U and (ii) the availability of an internal HF field in the AFM state of UO_2 of ∼252 T, giving a central frequency (i.e., the ± 1/2 transition) of 198 MHz for the AFNMR spectrum. At that frequency, even $\gamma_{235}/2\pi \sim 0.78$ MHz/T is large enough to provide a useable signal at helium temperatures.

With $I = 7/2$ and a sizeable quadrupole splitting, the spectrum consists of the central transition and six quadrupolar satellites, shown in Fig. 2 at a temperature of 1.5 K. The quadrupole splitting arises, because UO_2 also undergoes electric quadrupolar ordering along with magnetic dipolar ordering, as has been confirmed by resonant X-ray scattering [11]. Thus, the oblate quadrupolar moment is coaxial with the magnetic moment and becomes an integral part of the triple-q order in the magnetoquadrupolar ground state [12,13]. The uniform spacing of quadrupolar satellites is a consequence of an axial electric field gradient (EFG) tensor with an axis that coincides with the internal HF field. In such a case when the azimuthal component of angular momentum ($\langle I_z \rangle = m$) is diagonal, then so is the nuclear quadrupole interaction [14]

[1] In Ref. [1] it was necessary to estimate the magnitude of a Van Vleck NMR shift of ∼25% in order to calculate the value of the gyromagnetic ratio of ^{239}Pu. The resulting value of 2.29 MHz/T is subject to the uncertainty of that estimate.

Table 1
Electron configuration, ground multiplet, cubic crystal field ground state, and nuclear properties of the four actinide ions we are concerned with in this paper.

Actinide ion	Ground multiplet	Cubic CF gnd. state	Nuclear spin I	Gyromagnetic ratio γ (MHz/T)	Half life (years)
$^{235}U^{4+}(5f^2 6s^2 6p^6)$	$^3H_4$	Γ_5 [6]	7/2	0.78	7.0×10^8
$^{237}Np^{4+}(5f^3 6s^2 6p^6)$	$^4I_{9/2}$	Γ_8 [7]	5/2	9.57	2.4×10^6
$^{239}Pu^{4+}(5f^4 6s^2 6p^6)$	$^3H_4$	Γ_1 [8]	1/2	2.29	2.4×10^4
$^{243}Am^{4+}(5f^2 6s^2 6p^6)$	$^6H_{5/2}$	$\Gamma_{7,8}$ [9,10]	5/2	4.6	7.37×10^3

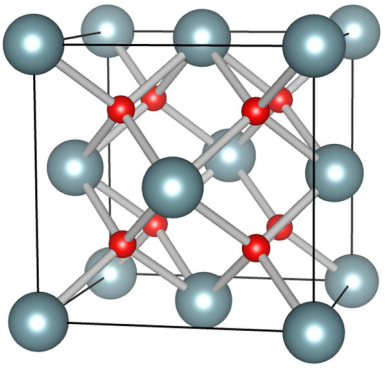

Fig. 1. (Color online.) The AnO_2 compounds all crystallize in the CaF_2 structure shown. Here the An^{4+} ions (blue spheres) occupy an fcc lattice, while the O^{2-} (red spheres) form an interpenetrating sc lattice with half the lattice parameter of the fcc lattice. Adapted from Ref. [3].

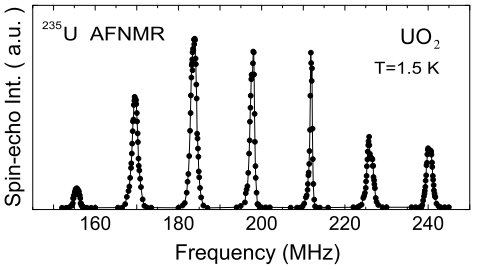

Fig. 2. Frequency scan of the integrated spin-echo amplitude over the AFNMR spectrum of ^{235}U in UO_2 at $T = 1.5$ K. Adapted from Ref. [3].

$$\langle m|\mathcal{H}_Q|m\rangle = \frac{1}{4}h\nu_Q\left(3\cos^2\theta - 1\right)\left(m^2 - I(I+1)\right), \quad \text{where } \nu_Q = \frac{3e^2qQ}{2hI(2I-1)} \tag{1}$$

and where q and Q are the principal components of the electric field gradient (EFG) and the nuclear quadrupole moment, respectively. From Eq. (1) one sees that there is a uniform frequency splitting of $(3\cos^2\theta - 1)\nu_Q/2$ between quadrupolar satellites. Since the field gradient axis is parallel to the HF field for ^{235}U (i.e. $\theta = 0$), the splitting is simply $\nu_Q \sim 14$ MHz.

Important results on the magnetic structure and dynamics of UO_2 have also been derived from properties of the ^{17}O NMR. The natural abundance of ^{17}O is a small fraction of 1%, so for UO_2 and other oxygen-bearing compounds NMR studies require artificial enrichment of this isotope, which has a nuclear spin $I = 5/2$ and $\gamma_{17}/2\pi = 5.7719$ MHz/T. The NMR line at 61.6 MHz in the paramagnetic state is shown in the inset to Fig. 3a, where it is seen to be symmetric with a width of about 30 G. There is no quadrupole splitting, and the shift (Fig. 3a) is isotropic, small and only slightly dependent on temperature. The symmetry of the oxygen sites in the paramagnetic state is cubic (see Fig. 1).

The spin–lattice relaxation rate $1/T_1$ is plotted as a function of temperature in Fig. 3b, where it is seen to execute a sharp increase with decreasing temperature just above the Nèel point, as though approaching a second-order phase transition. Eventually the transition goes first-order, as one can see from the discontinuity in T_1 at $T_N \simeq 30.8$ K.

The magnetically ordered state of UO_2 is a rare example of AFM ordering of moments on an fcc lattice. Early work predicted simple AFM order with spins along a coordinate axis [15]. Later neutron work revealed a more complex picture, with spin ordering either in the basal plane ($2k$) or along $\langle 111\rangle$ axes ($3k$) [16]. The $3k$ option is illustrated in Fig. 4. The $3k$ ordering scheme appears highly complex, but is actually straightforward (see caption to Fig. 4). Neutron data were unable to distinguish between these two, but modeling the observed EFG of the axial-site ^{17}O NMR line provided a resolution of this question (see below).

Before reviewing that argument, we describe the observed behavior of the ^{17}O NMR in the ordered state of UO_2. The neighboring ordered moments generate a transferred HF field $H_{int} \sim 0.74$ T, which in a powder sample will lie at some random angle θ to the applied field. The resonance condition can then be written $\omega_{NMR} = \gamma_{17}[H_0 + H_{int}\cos\theta]$. Thus, in a

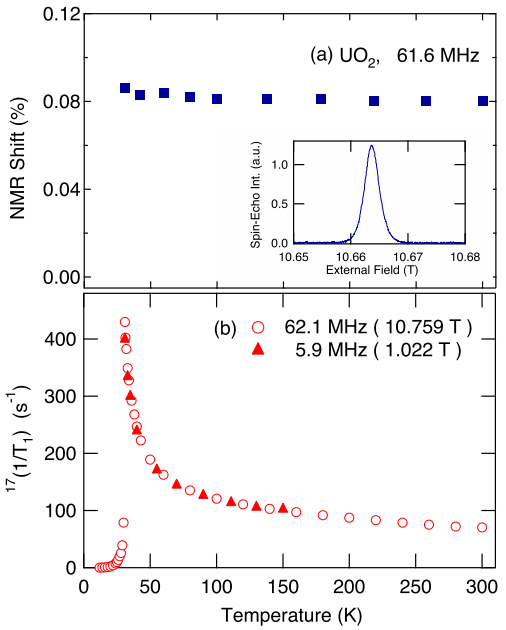

Fig. 3. (Color online.) (a) NMR shift of ^{17}O is plotted vs. temperature T in the paramagnetic state of UO_2. Inset shows a field scan of the ^{17}O NMR line at $f = 61.6$ MHz at a $T = 300$ K, exhibiting a width of ~ 30 G. (b) Temperature dependence of the ^{17}O nuclear spin–lattice relaxation rate $(1/T_1)$ at 62.1 MHz, showing what appears to be critical slowing down of fluctuations approaching T_N, followed by a sudden drop as the transition goes first order. Adapted from Ref. [3].

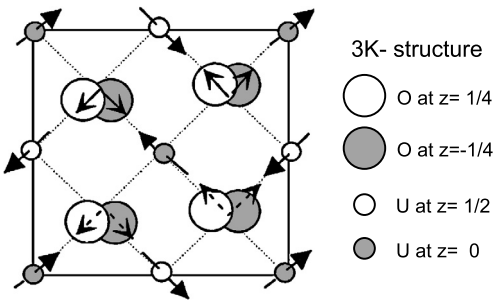

Fig. 4. The arrangement of antiferromagnetic sublattices that constitutes 3k AFM order in a (001) projection. The four sc lattices that make up the fcc crystal structure are each assigned one of the four ⟨111⟩ axes and a unique direction for the corresponding uranium moments (small circles). The directions are chosen so that the net moment ⊥ each coordinate plane is zero. The clear and shaded small circles indicate uranium sites in the $z = 1/2$ and $z = 0$ planes, respectively. The large circles indicate oxygen sites in the $z = 1/4$ (clear) and $z = -1/4$ (shaded) planes. The corresponding arrows indicate small JT displacements of oxygen ions along the indicated ⟨111⟩ axes, where dashed arrows indicate a downward displacement. Adapted from Ref. [3].

field scan, a continuous distribution of spin echo intensity can be recorded for fields in the range $H_0 - H_{\rm int} \leq \omega_{\rm NMR}/\gamma_{17} \leq H_0 + H_{\rm int}$. The result from such a scan is shown as a noisy trace near the bottom of Fig. 5.

Also observed in the ^{17}O NMR study was an oscillatory spin-echo decay pattern (not shown) [3]. This effect was identified as stemming from a small quadrupole splitting that occurs in the AFM state [17]. The splitting frequency is plotted as a function of $\cos\theta$ (θ = polar angle), with the result shown in Fig. 5 (dots). If we model this effect as an axial EFG, then using Eq. (1), one finds the splitting as a function of $\cos\theta$. The latter result is plotted as a solid curve scaled to the data points in Fig. 5, giving confirmation that the axial EFG is a reasonable assumption. Note that the measured modulation is a small fraction of the linewidth in Fig. 3a (inset). Calculations of the dipolar HF field in the ordered state show that for every site it lies along the local ⟨111⟩ axis, and further, a simple point-charge model of the EFG assuming the small Jahn–Teller displacements of the O^{2-} shown in Fig. 4 yields an axial EFG also lying along the local ⟨111⟩ axis. Meanwhile, the 2k structure gives a strongly non-axial EFG tensor in the same approximation. These results, compared with the findings in Fig. 5, give good evidence for the 3k structure in AFM-ordered UO_2.

Finally, we display and interpret spin–lattice relaxation time (T_1) data for both ^{235}U and ^{17}O taken in the AFM ordered state of UO_2. T_1 data for both nuclear species are shown in Fig. 6, obtained over temperatures ranging from 4.2 K to 14.5 K for ^{235}U and from 12 K up to 50 K for ^{17}O (recall that T_1 data for ^{17}O in Fig. 3 extends up to 300 K). The data in Fig. 6 make clear the ordered-state behavior of spin–lattice relaxation in UO_2, namely $1/T_1 \propto T^7$ up to temperatures near T_N, with a slight increase above T^7 just before it makes a first-order jump to the paramagnetic state. In effect, then, the T^7

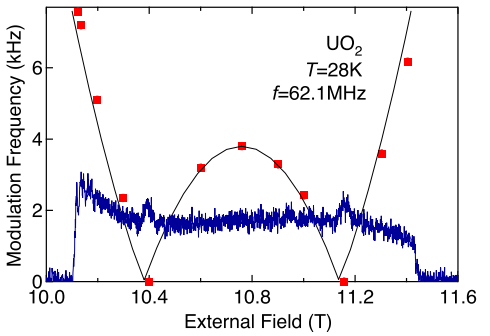

Fig. 5. (Color online.) The noisy trace at the bottom shows a field scan of the ^{17}O nuclear spin echo amplitude in the AFM state at 28 K and a frequency of 62.1 MHz. The width of the spectrum is $2H_{\rm int}$ with a scale $\propto H_{\rm int}\cos\theta$. The corresponding quadrupolar splittings, reflected in spin echo oscillations (see text), are shown as red squares. The solid line is the theory curve $\nu_{\rm Q}|3\cos^2\theta - 1|$ adjusted to fit the data points (see vertical scale). Adapted from Ref. [3].

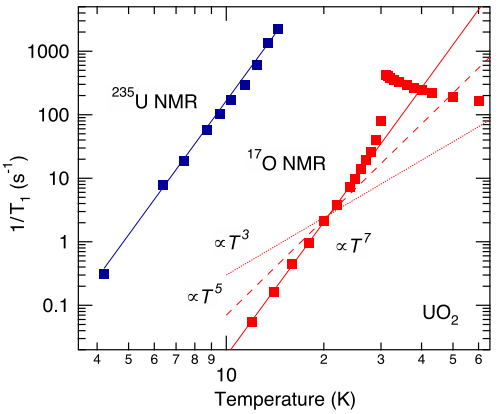

Fig. 6. (Color online.) Data for the spin-lattice relaxation rates $1/T_1$ of both ^{235}U and ^{17}O in UO_2 are shown plotted vs. temperature on a log–log scale. The solid lines drawn show that HF-field fluctuations for these two nuclear species obey a $\sim T^7$ law over, collectively, many orders of magnitude. Such relaxation behavior was shown many years ago to arise in ordered magnets from a phonon Rahman process combined with strong magneto-elastic coupling [18]. The contrast between $1/T_1$ values for ^{235}U and ^{17}O shows that fluctuating HF fields at the magnetic ion and at the ligands in this case differ by nearly three orders of magnitude. Adapted from Ref. [3].

relaxation process persists over five orders of magnitude. Such a temperature characteristic does not correspond to any known magnon-scattering process *per se*, but was identified many years ago as a phonon Raman process effecting relaxation through magneto-elastic coupling in the system [18]. The ratio of the T_1 values for the two nuclear species measured is very nearly 10^4, revealing that the ratio of effective fluctuating HF fields is $H_{\rm HF}(235)/H_{\rm HF}(17) \simeq 100$ $(\gamma_{17}/\gamma_{235}) = 736$. Thus, HF coupling for the uranium ion is nearly three orders of magnitude greater than for the oxygen ligand. This ratio was found to be of the order of magnitude expected for actinide ions [3].

The comprehensive study of actinide/ligand NMR in UO_2 settled the question of its AFM ordering structure and set the stage for investigation of other actinide compounds as well. Its properties, however, were only the beginning of the interesting surprises to come in the continuing investigation of actinide oxides.

3. ^{17}O NMR study of NpO_2 confirms a multipolar ground state

With the same fluorite structure and stronger paramagnetism of NpO_2, as compared with UO_2, a tentative, but mistaken conclusion was broached that NpO_2 also underwent AFM ordering [21]. A comparative study of magnetic susceptibility for these two systems showed remarkably similar behavior, with NpO_2 having a somewhat larger effective moment in the paramagnetic state [19,20]. The specific heat curves for these two systems are also strikingly similar [21], showing clear lambda anomalies at 26 K and 30.8 K for NpO_2 and UO_2, respectively. Surprisingly, neither Mössbauer [22] nor neutron studies [24] showed a dipole moment to be present at $T < T_0$ for NpO_2. This question remained unresolved for nearly fifty years.

In 2000, Santini and Amoretti [20] summarized current experimental evidence and proposed a Γ_2 ground state that would carry an octupolar moment. This was followed quickly by seminal resonant X-ray scattering results by Paixão et al., which, surprisingly, showed strong quadrupolar scattering, in apparent contradiction of the octupolar moment proposal [7]. Either way, this would lead to the first case of actinide multipolar ordering. One final ingredient to this mix was the

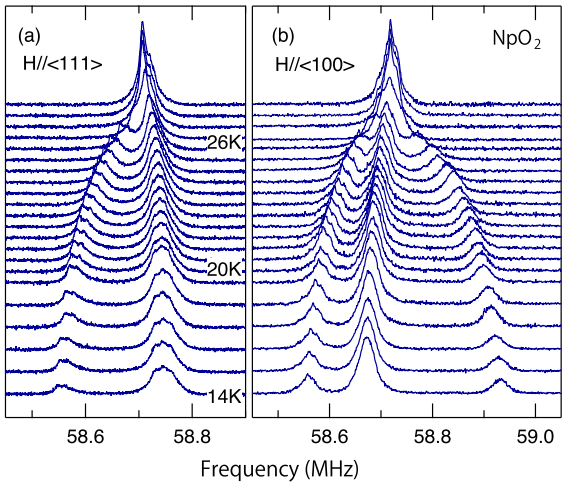

Fig. 7. Integrated ^{17}O spin-echo spectroscopy data are plotted vs. frequency for applied field along the (a) ⟨111⟩ and (b) ⟨110⟩ axis of a single-crystal sample. Vertically, there is a series of scans at temperatures ranging from above T_N at the top down to 14 K at the bottom. These data illustrate the development of anisotropic NMR shifts as the system undergoes octupolar and quadrupolar magnetic ordering below $T_0 \simeq 26$ K. The measured shifts confirm the expected behavior of triple-q multipolar ordering as discussed in the text. Adapted from Ref. [28].

observation of a strong interstitial magnetic field at $T < T_0$ by means of μSR [25], confirming that this system has a ground state that breaks time reversal symmetry.

The RXS results led to the following scenario: the 5f electrons of the Np^{4+} were proposed to form octupole moments in an arrangement with the four [111] axes forming a triple-q array not unlike the 3k ordering of magnetic moments in the AFM state of UO_2. As a secondary order parameter, quadrupole moments would develop along the same set of triple-q axes. This combination is permitted by a Γ_8 crystal field ground state. It accounted for the quadrupole-dominated RXS data and allowed for breaking of time-reversal symmetry, while the cubic lattice remains undisturbed [26]. Interestingly, an octupolar contribution to the RXS data was predicted to occur, but was simply too weak to be observed. And as the authors emphasized, it was a proposal that needed verification by a microscopic probe [7].

Following the work described, oxygen NMR studies with, first, powder specimens [27] and then with a single crystal [28], both doped with a generous concentration of the rare isotope ^{17}O, were launched to test the microscopic features of the proposed triple-q ordering arrangement. We discuss the results of these studies here in some detail [27,28]. At the outset we review the local symmetry of the oxygen sites. First, in the paramagnetic state, the crystal has the cubic space group (SG) $Fm\bar{3}m$, and all oxygens occupy equivalent '8c' positions. With triple-q order, the crystal symmetry is lowered to SG $Pn\bar{3}m$. The fcc lattice of Np^{4+} sites is divided into four interpenetrating sc lattices. Each one of these sc lattices is associated with one of the four ⟨111⟩ axes in the structure, giving all corresponding Np^{4+} sites a symmetry axis. With Np^{4+} sites so assigned, the result is the longitudinal triple-q structure. As for the oxygens, each fcc unit cell contains eight oxygen sites, each of which is at the center of a tetrahedron of Np^{4+} sites (see Fig. 1). Of those eight, two (2a) oxygen sites retain cubic symmetry and six (6d) sites are lowered to axial symmetry. Here we denote these the $O^{(1)}$ (cubic) and the $O^{(3)}$ (axial) sites. Two axial sites in each unit cell have (x, y, z) respective symmetry axes, which we further denote as the $O_x^{(3)}$, $O_y^{(3)}$, and $O_z^{(3)}$ sites.

In experimental NMR spectra, the $O^{(1)}$ site will have an isotropic NMR shift and the $O^{(3)}$ sites will have axial NMR shift tensors, one with each of the three (x, y, z) symmetry axes. In Fig. 7 we exhibit NMR spectra at a series of temperatures with the applied field along particular directions to test the hypothesis of triple-q ordering. In Fig. 7(a), the field is along a ⟨111⟩ axis, so that the three axial sites are equivalent and are seen to form a composite NMR line below T_0 as expected. The cubic site has a distinct shift, so there are two lines with intensity 3:1, in accord with triple-q ordering. In Fig. 7(b), the field is along a ⟨110⟩ axis, so that $O_x^{(3)}$ and $O_y^{(3)}$ are equivalent, but $O_z^{(3)}$ and $O^{(1)}$ are distinct. As expected, there are now three NMR lines, two of the same weight and one with twice that weight. Moreover, the $O^{(1)}$ line is in the same place for both field orientations in accord with its expected isotropic shift. Thus, NMR shifts corroborate the 3:1 partition of the ^{17}O NMR spectrum expected for triple-q quadrupolar order.

In an extension of this type of argument, Sakai, Shina, and Shiba [23] have done a symmetry-based analysis of the field-induced NMR shift behavior that is possible with triple-q antiferro-octupolar/antiferro-quadrupolar (AFO/AFQ) order in NpO_2. These results, along with zero-field effects, are summarized in Table 2. The top line in the table gives the type of multipole, first for zero field, then field-induced (FI) effects. The second line gives the coefficients (c.c.) that are defined in the source paper, and lines 3–6 give the form of expected results for the four oxygen sites. In the fourth column of results the O_{ij}'s are coefficients for field-induced quadrupole effects, and in the fifth column results are given for two types ('T^{β}' and 'T_{xyz}') of field-induced octupole moments.

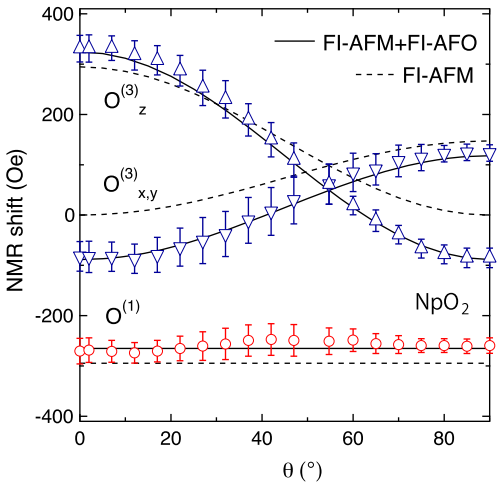

Fig. 8. (Color online.) ^{17}O NMR shifts are shown for the three axial-symmetry and one cubic-symmetry sites in NpO_2, which are plotted vs. polar angle θ on a scan of **H** from the ⟨001⟩ axis to the ⟨110⟩ axis as described in the text. These shifts are fitted to and found to agree with the symmetry-based theory by Sakai, Shiina and Shiba, including field-induced antiferromagnetic and octupolar moments (see text) [23]. The dashed lines illustrate the marked deterioration of the fit that occurs when the field-induced octupolar terms are omitted. Adapted from Ref. [28].

Table 2
Possible HF interactions with O nuclei in the longitudinal triple-q AFO/AFQ ordered state. The definitions of coupling constants (c.c.) are given in [23]. $\mathbf{q}_z$ is the principal axis of the EFG tensor.

Item	$\mathbf{H}=0$		$\mathbf{H}=(H_x,H_y,H_z)$		
Multipole	AFO	AFQ	FI–AFM	FI–AFQ	FI–AFO (T^{β}/T_{xyz})
c.c.	$C_{1,1}$	$C_{2,2}$	$2C_{1,2}$	$C_{2,5}$	$-2C_{1,3}/C_{1,4}$
$O^{(1)}$	0	0	(H_x, H_y, H_z)	0	$(0,0,0)/(H_x, H_y, H_z)$
$O^{(3)}_z$	0	$\mathbf{q}_z \parallel [001]$	$(0,0,-H_z)$	$[O_{yz}H_x + O_{zx}H_y]$	$(H_x,H_y,0)/(-H_x,-H_y,H_z)$
$O^{(3)}_y$	0	$\mathbf{q}_z \parallel [010]$	$(0,-H_y,0)$	$[O_{xy}H_z + O_{yz}H_x]$	$(H_x,0,H_z)/(-H_x,H_y,-H_z)$
$O^{(3)}_x$	0	$\mathbf{q}_z \parallel [100]$	$(-H_x,0,0)$	$[O_{zx}H_y + O_{xy}H_z]$	$(0,H_y,H_z)/(H_x,-H_y,-H_z)$

Using results from Table 2, it was shown that the NMR shift data actually confirm the existence of field-induced octupole moments. First, we comment on each column in the table, starting on the left. Under AFO there are no zero-field HF effects from the octupolar ground-state moment. Any such effects (e.g., magnetic fields) are zero at points of high symmetry in the lattice. However, as noted earlier, μSR observations of interstitial magnetic fields in the AFO/AFQ ground state have been reported for NpO_2 [25]. A related effect having to do with lattice distortions from impurities, etc., is discussed below. In the next column it is noted that a small EFG appears along the symmetry axis of the three axial oxygen sites in the AFO/AFQ state. There is no lattice distortion, so the cubic structural symmetry is retained; the axial EFG's result from AFQ ordering. The fourth column specifies the form of NMR shifts resulting from field-induced AFM moments; these are discussed in detail below. In the fifth column allowed field-induced quadrupole (EFG) energies are specified; these were not large enough to be resolved in the measurements reported in [28]. The last column spells out the form of HF energies that result from field-induced octupole moments. These combine with the FI–AFM effects in column four to yield the NMR shifts below T_0 that are illustrated in Fig. 8.

The latter shift data are obtained by scanning the polar angle θ from 0, where $\mathbf{H} \parallel [001]$, down to $\theta = \pi/2$ where $\mathbf{H} \parallel [110]$, passing through the [111] axis en route. The field components for this scan may be written $\mathbf{H} = (H_x, H_y, H_z) = H(\sin\theta/\sqrt{2}, \sin\theta/\sqrt{2}, \cos\theta)$. Shift data for the three lines in the ^{17}O NMR spectrum are plotted in Fig. 8 for the θ scan described. To interpret these data we construct, for each oxygen site, a total shift expression from the terms in Table 2 in the FI–AFM and FI–AFO columns, with each projected onto the field orientation unit vector $(\sin\theta/\sqrt{2}, \sin\theta/\sqrt{2}, \cos\theta)$. The following expressions for the three curves in Fig. 8 are obtained:

$$\begin{aligned}
\Delta H_1 &= [2C_{1,2} + C_{1,4}]H \\
\Delta H_{3xy} &= \left[-C_{1,2}\sin^2\theta - C_{1,3}\left(1+\cos^2\theta\right) - C_{1,4}\cos^2\theta\right]H \\
\Delta H_{3z} &= \left[-2C_{1.2}\cos^2\theta - 2C_{1,3}\sin^2\theta + C_{1,4}\left(2\cos^2\theta - 1\right)\right]H
\end{aligned} \tag{2}$$

The solid lines in the figure result from fitting these three equations to the data, with parameters adjusted as follows: $C_{1,2}H = -143.7$ Oe, $C_{1,3}H = C_{1,4}H = 29.5$ Oe. An excellent fit to the entire data set within the error bars is achieved with just these three parameters. Moreover, the octupolar terms make an important contribution to these fits; thus, the quality of the fits is grossly degraded if the latter terms are omitted (dashed lines in Fig. 8). It is interesting to note that according

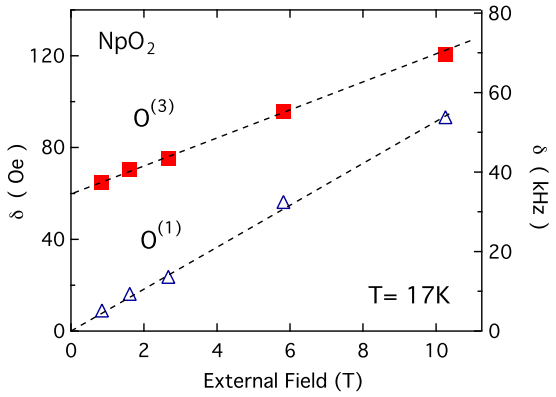

Fig. 9. (Color online.) ^{17}O NMR line broadening parameters δ are plotted as a function of applied field H at $T = 17$ K for the cubic site (filled circles) and the combined axial sites (open circles). The cubic site linewidth is seen to extrapolate to zero as $H \to 0$ as expected. The axial site broadening, on the other hand, extrapolates to a finite value of 60 gauss. This behavior confirms the presence of ordered magnetic moments, described by Santini and Amoretti as "tiny moment antiferromagnetism", throughout the sample [20]. See text for further discussion. Adapted from Ref. [27].

to recent calculations and experiments, the rank 5 term is the dominant multipole in NpO_2 [29–31]. What field-induced HF effects such a term would give rise to is not known at the present time.

Thus, the expected consequences of AFQ/AFO ordering in NpO_2 are borne out as far as the ^{17}O NMR spectra are concerned. A further confirmation of multipolar ordering for this system emerges from a surprising phenomenon, namely the observation of stray, fixed magnetic moments. This effect came to light in the study of ^{17}O NMR shift variation as a function of applied magnetic field in earlier work on a powdered sample [27]. The ^{17}O NMR spectrum in this case was a single line for the $O^{(1)}$ site and a composite powder-pattern arising from the anisotropic shifts of the $O^{(3)}$ sites (see Eq. (2)). Each of these elements was further broadened by the effects of disorder in the powder sample. The latter effects were well accounted for by convolution with Gaussian 'broadening functions' having width parameters δ, one each for the $O^{(1)}$ and $O^{(3)}$ spectral features. What is interesting is the behavior of the δ values as a function of the applied field shown in Fig. 9. While δ for the $O^{(1)}$ cubic site extrapolates quite precisely to a zero value as $H \to 0$, δ for the $O^{(3)}$ axial sites quite clearly approaches a finite value at zero applied field. This is only possible if there are small, fixed magnetic moments distributed throughout the volume of the sample. Thus, this linewidth effect is identified as 'tiny moment antiferromagnetism'; this was described by Santini and Amoretti in their proposal of an octupolar ground state in NpO_2 [20]. These authors note that the occurrence of small trigonal strains in the NpO_2 unit cell can generate small moments that account for the occurrence of Mössbauer line broadening in this system in zero applied field. They attribute it directly to the time-reversal symmetry-breaking of the OP, and thus to the octupolar ground state.

Finally, we mention in passing that values of T_1 (∼40 ns) for the ^{237}Np nuclear spins have been estimated through analysis of a cross-relaxation effect that fluctuations of the ^{237}Np spins have on the measured ^{17}O spin–lattice relaxation in the paramagnetic state of NpO_2 [32]. Interestingly, the observed cross relaxation is only made possible through the agency of ^{237}Np–^{17}O indirect spin–spin coupling that first came to light with these measurements. The latter coupling appears to be limited to 5f electron systems [33].

4. NMR studies of PuO_2 and AmO_2

After many years of effort to observe the NMR of ^{239}Pu, this elusive prize was recently reported by Yasuoka and coworkers for the host compound PuO_2 [1]. In this system the Pu^{4+} has a nonmagnetic Γ_1 singlet ground state. The difficulty in resolving the ^{239}Pu NMR signal in such a case stems from the absence of any intrinsic T_1 mechanism in a non-magnetic host; one has, instead, to rely on the presence of paramagnetic impurities and nuclear spin diffusion. The line was found to be fairly broad, and extraction of the gyromagnetic ratio γ_{239} required an estimate of a Van Vleck paramagnetic shift amounting to $\sim 25\%$. The value $\gamma_{239} = 2.29$ MHz/T was arrived at with the latter shift estimate. Fluctuations in the value of such a shift are more than likely a source of line broadening. Nonetheless, the PuO_2 NMR study goes a long way toward making ^{239}Pu NMR a resource in the study of plutonium compounds.

Meanwhile, a preliminary study of ^{17}O NMR in a well-aged sample of $^{243}AmO_2$ was reported some time ago [34]. Recently, a study was conducted on a fresh sample just a few weeks old. It was found that already after 13 days the sample exhibited what appears to be a spin-glass transition at $T \simeq 8.5$ K. At $T = 1.5$ K, the ^{17}O NMR spectrum in Fig. 10 shows a small, narrow line on top of an extremely broad line with more than 90% of the intensity. The narrow line is of a similar width to the ^{17}O spectrum in the paramagnetic state. Such lines are narrow, because the magnetic polarization is entirely due to the applied field; dipolar HF fields from field-induced magnetization tend to cancel out because of cubic local symmetry. If the 5f magnetic moments become frozen in random directions through magnetic frustration and disorder, the very large transferred dipolar HF fields at the ^{17}O sites become "activated", because the cancellation by symmetry is no

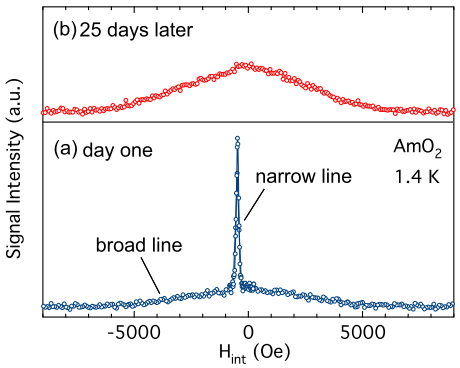

Fig. 10. (Color online.) (a) The ^{17}O NMR spectrum in $^{243}AmO_2$ at $T = 1.4$ K on day one of NMR studies (thirteen days after synthesis) is seen to consist of a narrow line characteristic of the paramagnetic phase and a very broad line found in the spin-glass phase at $T < 8.5$ K. (b) 25 days later the narrow line has disappeared and only the slightly strengthened wide line remains. We interpret this to mean that the entire sample has now been converted to a highly disordered state by nuclear decay recoil processes of the $^{243}Am^{4+}$ ions. See text for further interpretive comments. Adapted from Ref. [35].

longer effective. This unleashes a huge broadening mechanism, which is believed to cause the linewidth of several kilogauss seen in Fig. 10.

One is not surprised by the presence of disordered material in AmO_2, because the shortness of the half-life of ^{243}Am will always cause such regions to develop in the sample. What is surprising are two things: (i) first, that after only 13 days at room temperature following synthesis, more than 90% of the sample material is already converted to a highly disordered spin glass phase, and (ii) that some of the material can remain in what appears to be a paramagnetic state down to 1.5 K, while exchange couplings as reflected in the Curie–Weiss temperature are clearly of the order of tens of degrees. The nominal ground state of Am^{4+} is a Γ_7 doublet capable only of dipolar ordering. It has, however, been pointed out more recently that through competition between spin–orbit coupling and Coulomb interactions it is possible that a Γ_8 quartet lies lowest. In that event, quadrupolar and octupolar ground states are also possible [10]. Shortly after the data in Fig. 10 were taken, the paramagnetic line seen in the figure disappeared, after which all of the material either exhibits the broad linewidth seen there or has had its NMR signal 'wiped out' by slowly fluctuating, giant HF fields. More detail about the behavior of this sample is revealed in a recently published paper [35].

5. Summary

NMR studies of the ^{17}O ligand nuclei in actinide oxides have been seen to offer a window of observation on precisely what is going on in the low-temperature states of these systems. Questions such as the magnitude, symmetry and fluctuation intensity of magnetism may be probed in this way, and even the notoriously difficult rank 3 and 5 magnetic multipoles that induce no magnetic fields at neighboring cubic-site ligands can be probed through the effects of secondary order parameters. A good example is the triple-q quadrupolar order in NpO_2. We also note that recent calculations suggest that the rank 5 multipole is actually dominant in the NpO_2 ground state [29–31]. The study of such effects is also a good model for the study of more mysterious low-temperature phenomena in other actinide systems. A good example is the ever-elusive case of URu_2Si_2 [36,37].

Acknowledgements

We would like to thank Drs. H. Sakai, K. Ikushima, H. Yasuoka, S. Tsutsui, S. Nasu, A. Nakamura, Y. Homma, D. Aoki, Y. Shiokawa, T. Nishi. M. Nakata. A. Itho, Y. Haga, Y. Ōnuki, T. Hotta, K. Kubo for collaboration and fruitful discussion in the study of actinide dioxides. A part of this work was supported by a Grant-in-Aid for Young Scientists (A) [No. 23686137] by the Japan Society for the Promotion of Science (JSPS), and a Grant-in-Aid for Scientific Research on Innovative Areas "Heavy Electrons" [Nos. 20102006, 20102007] by the Ministry of Education, Culture, Sports, Science, and Technology of Japan, and the REIMEI Research Program of JAEA.

References

[1] H. Yasuoka, G. Koutroulakis, H. Chudo, S. Richmond, D.K. Veirs, A.I. Smith, E.D. Bauer, J.D. Thompson, G.D. Jarvinen, D.L. Clark, Observation of ^{239}Pu nuclear magnetic resonance, Science 336 (2012) 901–904.

[2] K. Ikushima, H. Yasuoka, S. Tsutsui, M. Saeki, S. Nasu, M. Date, Observation of ^{235}U NMR in the antiferromagnetic state of UO_2, J. Phys. Soc. Jpn. 67 (1998) 65–66.

[3] K. Ikushima, S. Tsutsui, Y. Haga, H. Yasuoka, R.E. Walstedt, N.M. Masaki, A. Nakamura, S. Nasu, Y. Ōnuki, First-order phase transition in UO_2: ^{235}U and ^{17}O NMR study, Phys. Rev. B 63 (2001) 104404, 10 p.

[4] Y. Tokunaga, Y. Homma, S. Kambe, D. Aoki, H. Sakai, H. Chudo, K. Ikushima, E. Yamamoto, A. Nakamura, Y. Shiokawa, R.E. Walstedt, H. Yasuoka, NMR investigation of quadrupole order parameter in actinide dioxides, J. Optoelectron. Adv. Mater. 10 (2008) 1663–1665.

[5] P. Santini, S. Carretta, G. Amoretti, R. Caciuffo, N. Magnani, G.H. Lander, Multipolar interactions in f-electron systems: the paradigm of actinide oxides, Rev. Mod. Phys. 81 (2009) 807.
[6] H.U. Rahman, W.A. Runciman, A crystal field calculation in uranium dioxide, J. Phys. Chem. Solids 27 (1966) 1833–1836.
[7] J.A. Paixão, C. Detlefs, M.J. Longfield, R. Caciuffo, P. Santini, N. Bernhoeft, J. Rebizant, G.H. Lander, Triple-q octupolar ordering in NpO_2, Phys. Rev. Lett. 89 (2002) 187202, 4 p.
[8] S. Kern, R.A. Robinson, H. Nakotte, G.H. Lander, B. Cort, P. Watson, F.A. Vigil, Crystal-field transition in PuO_2, Phys. Rev. B 59 (1999) 104–106.
[9] D.G. Karraker, Magnetic susceptibility of $^{243}AmO_2$, J. Chem. Phys. 63 (1975) 3174–3175.
[10] T. Hotta, Microscopic analysis of multipole susceptibility of actinide dioxides: a scenario of multipole ordering in AmO_2, Phys. Rev. B 80 (2009) 024408, 7 p.;
T. Hotta, H. Harima, Effective crystalline electric field potential in a j–j coupling scheme, J. Phys. Soc. Jpn. 75 (2006) 124711, 15 p.
[11] S.B. Wilkins, R. Caciuffo, C. Detlefs, J. Rebizant, E. Colineau, F. Wastin, G.H. Lander, Direct observation of electric-quadrupolar order in UO_2, Phys. Rev. B 73 (2006) 060406, 4 p.
[12] S. Carretta, P. Santini, R. Caciuffo, G. Amoretti, Quadrupolar waves in uranium dioxide, Phys. Rev. Lett. 105 (2010) 167201, 4 p.
[13] R. Caciuffo, P. Santini, S. Carretta, G. Amoretti, A. Hiess, N. Magnani, L.-P. Regnault, G.H. Lander, Multipolar, magnetic, and vibrational lattice dynamics in the low–temperature phase of uranium dioxide, Phys. Rev. B 84 (2011) 104409, 10 p.
[14] A. Abragam, Principles of Nuclear Magnetism, Clarendon Press, Oxford, 1961, p. 233.
[15] S.J. Allen, Spin–lattice interaction in UO_2. I. Ground-state and spin-wave excitations, Phys. Rev. 166 (1968) 530–539;
R.A. Cowley, G. Dolling, Magnetic excitations in uranium dioxide, Phys. Rev. 167 (1968) 464–477.
[16] J. Faber Jr., G.H. Lander, Neutron diffraction study of UO_2: antiferromagnetic state, Phys. Rev. B 14 (1976) 1151–1164;
P. Burlet, J. Rossat-Mignod, S. Quezel, O. Vogt, J.C. Spirlet, J. Rebizant, Neutron diffraction on actinides, J. Less-Common Met. 121 (1986) 121–139.
[17] H. Abe, H. Yasuoka, A. Hirai, Spin echo modulation caused by the quadrupole interaction and multiple spin echoes, J. Phys. Soc. Jpn. 21 (1966) 77–89.
[18] P. Pincus, J. Winter, Influence of magnon–phonon coupling on the low-temperature magnetic properties of an antiferromagnet, Phys. Rev. Lett. 7 (1961) 269–270.
[19] J.W. Ross, D.J. Lam, The magnetic susceptibility of neptunium oxide and carbide between 4.2 K and 350 K, J. Appl. Phys. 38 (1967) 1451–1453.
[20] P. Santini, G. Amoretti, Magnetic-octupole order in neptunium oxide? Phys. Rev. Lett. 85 (2000) 2188–2191.
[21] D.W. Osborne, E.F. Westrum Jr., The heat capacity of thorium dioxide from 10 to 305° K. The heat capacity anomalies in uranium dioxide and neptunium dioxide, J. Chem. Phys. 21 (1953) 1884–1887.
[22] J.M. Friedt, F.J. Litterst, J. Rebizant, 25-K phase transition in NpO_2 from ^{237}Np Mössbauer spectroscopy, Phys. Rev. B 32 (1985) 257–263.
[23] O. Sakai, R. Shiina, H. Shiba, Invariant form of hyperfine interaction with multipolar moments – observation of octupolar moments in NpO_2 and $Ce_{1-x}La_xB_6$ by NMR, J. Phys. Soc. Jpn. 74 (2005) 457–467.
[24] R. Caciuffo, G.H. Lander, J.C. Spirlet, J.M. Fournier, W.F. Kuhs, A search for anharmonic effects in NpO_2 at low temperature by neutron diffraction, Solid State Commun. 64 (1987) 149–152.
[25] W. Kopmann, F.J. Litterst, H.-H. Klauss, M. Hillberg, W. Wagener, G.M. Kalvius, E. Schreier, F.J. Burghart, J. Rebizant, G.H. Lander, Magnetic order in NpO_2 and UO_2 studied by muon spin rotation, J. Alloys Compd. 271–273 (1998) 463–466.
[26] D. Mannix, G.H. Lander, J. Rebizant, R. Caciuffo, N. Bernhoeft, E. Lidström, C. Vettier, Unusual magnetism of NpO_2: a study with resonant X-ray scattering, Phys. Rev. B 60 (1999-II) 15187–15193.
[27] Y. Tokunaga, Y. Homma, S. Kambe, D. Aoki, H. Sakai, E. Yamamoto, A. Nakamura, Y. Shiokawa, R.E. Walstedt, H. Yasuoka, NMR evidence for triple-q multipole structure in NpO_2, Phys. Rev. Lett. 94 (2005) 1372091, 4 p.
[28] Y. Tokunaga, D. Aoki, Y. Homma, S. Kambe, H. Sakai, S. Ikeda, T. Fujimoto, R.E. Walstedt, H. Yasuoka, E. Yamamoto, A. Nakamura, Y. Shiokawa, NMR evidence for higher-order multipole order parameters in NpO_2, Phys. Rev. Lett. 97 (2006) 2576011, 4 p.
[29] P. Santini, S. Carretta, N. Magnani, G. Amoretti, R. Caciuffo, Hidden order and low-energy excitations in NpO_2, Phys. Rev. Lett. 97 (2006) 2072031, 4 p.
[30] N. Magnani, S. Carretta, R. Caciuffo, P. Santini, G. Amoretti, A. Hiess, J. Rebizant, G.H. Lander, Inelastic neutron scattering study of the multipolar order parameter in NpO_2, Phys. Rev. B 78 (2008) 104425, 6 p.
[31] T. Suzuki, N. Magnani, P. Oppeneer, First-principles theory of multipolar order in NpO_2, Phys. Rev. B 82 (2010) 241103R, 4 p.
[32] Y. Tokunaga, R.E. Walstedt, Y. Homma, D. Aoki, S. Kambe, H. Sakai, T. Fujimoto, S. Ikeda, E. Yamamoto, A. Nakamura, Y. Shiokawa, H. Yasuoka, ^{237}Np–^{17}O cross relaxation in NpO_2 driven by indirect spin-spin coupling, Phys. Rev. B 74 (2006) 064421, 7 p.
[33] H. Chudo, Y. Tokunaga, S. Kambe, H. Sakai, Y. Haga, T.D. Matsuda, Y. Ōnuki, H. Yasuoka, S. Aoki, Y. Homma, R.E. Walstedt, ^{237}Np nuclear relaxation rate in heavy fermion superconductor $NpPd_5Al_2$, Phys. Rev. B 84 (2011) 099402, 5 p.
[34] Y. Tokunaga, T. Nishi, S. Kambe, M. Nakada, A. Itoh, Y. Homma, H. Sakai, H. Chudo, NMR evidence for the 8.5 K phase transition in Americium oxide, J. Phys. Soc. Jpn. 79 (2010) 0537051, 4 p.
[35] Yo Tokunaga, T. Nishi, M. Nakada, A. Itoh, H. Sakai, S. Kambe, Y. Homma, F. Honda, D. Aoki, R.E. Walstedt, Self-radiation effect and glassy nature of magnetic transition in AmO_2 revealed by ^{17}O NMR, Phys. Rev. B 89 (2014) 214416, 8 p.
[36] S. Takagi, S. Ishihara, M. Yokoyama, H. Amitsuka, Symmetry of the hidden order in URu_2Si_2 from nuclear magnetic resonance studies, J. Phys. Soc. Jpn. 81 (2012) 114710, 13 p.
[37] S. Kambe, Y. Tokunaga, H. Sakai, T.D. Matsuda, Y. Haga, Z. Fisk, R.E. Walstedt, NMR study of in-plane twofold ordering in URu_2Si_2, Phys. Rev. Lett. 110 (2013) 246406, 4 p.